Empirical Model for Estimating the Exergy of Solar Radiation in Chile

Eduardo Rodríguez[1], Cristóbal Sarmiento[1] and José M. Cardemil[1]

[1] Mechanical Engineering Department, Universidad de Chile, Santiago (Chile)

Abstract

Exergy is a thermodynamic property that represents the potential work that can be delivered by a system. In that regard, the exergy of solar radiation could constitute a supporting tool for assessing the potential locations for the deploying of new solar energy project, as well as for evaluating the technologies to be considered. The present work, proposes an empirical model for the exergy of solar radiation, using meteorological data measured in Santiago, Chile. The developed model considers the clearness index as input variable, allowing to be applied throughout the country, using the satellite based global radiation estimations. Thirteen different models were analyzed in a regression routine, evaluating its effectiveness, and selecting the best approximation. An innovative experiment was also carried out, which allowed to verify the empirical model and compare it with other models proposed in the literature. The experiment follows the guideline of a test rig reported in the literature, which considers a photovoltaic panel and several sensors that allow to assess an accurate energy (and exergy) balance.

Keywords: Direct Radiation, Diffuse Radiation, Sky-Clearness Index, Exergy, Chile

1. Introduction

During recent years it has increased the global awareness about the environmental impact of human activities on the planet. Nowadays, as the citizens handle more information, they can discern about changing habits for the benefit of the environment. In this context, environmental awareness has propelled the deployment of several solar energy projects in Chile, allowing to diversify its energy matrix (Raugei et al., 2018). Chile presents outstanding conditions for developing solar energy systems, like the Atacama Desert in the northern region, which stands-out as one of the places with highest radiation worldwide (Escobar et al., 2015). Nowadays there are several new solar projects that are been developed thanks to the favorable conditions that the recent governments have promoted.

The quantification of the maximum amount of work that can be extracted from solar radiation still constitutes an active open discussion, as new materials are tested, and the limits of energy conversion are constantly pushed forward. Therefore, considering the availability and the intensity of solar radiation it is fundamental to determine the upper bound for the conversion efficiencies. In that regard, exergy is a property which represents the magnitude of the maximum useful work that can be extracted from any source of energy. The exergy of solar radiation has been studied since the '60s when Petela (Petela, 1964) proposed an initial model, which considers the Sun as a black body that emits radiation at a temperature T_s equivalent to the observed at the photosphere surface (5777 K).

$$\psi = 1 + \frac{1}{3}\left(\frac{T_0}{T_s}\right)^4 - \frac{4}{3}\frac{T_0}{T_s} \quad \text{(eq. 1)}$$

where ψ represent the maximum work obtainable from solar radiation and T_0 is the ambient temperature. Over the years, new models have been presented to estimate the exergy of solar radiation, among the models proposed stands-out those proposed by Jeter (Jeter, 1981), Gribik and Osterle (Gribik, J.A., Osterle, 1984) and Zamfirescu & Dincer (Zamfirescu and Dincer, 2009), which introduce significant changes to the original Petela's model (Petela, 1964), as observed in the following equation,

$$\psi = 1 - \frac{T_0}{T_s}\frac{I_{sc}}{I_{T0}} \quad \text{(eq. 2)}$$

doi:10.18086/swc.2019.45.08 Available at http://proceedings.ises.org

where I_{sc} is the solar constant and I_{T0} is the direct normal irradiance. Nevertheless, these models do not consider a specific term for computing the entropy generation when the radiation meets the terrestrial atmosphere, neither considered splitting the exergy of solar radiation in its direct and diffuse components. Later, Pons (Pons, 2012) managed to introduce these terms in a model that is able to assess the exergy of direct and diffuse radiation separately, and considers the entropy generation, based on the following definition of exergy:

$$B = E - T_0 S \quad \text{(eq. 3)}$$

where B is the exergy, E the amount of energy emitted by the source, T_0 the ambient temperature and S the entropy generated. Considering Pons's model (2012) and the empirical models of Jamil and Bellos (Jamil and Bellos, 2019), it is proposed in this work to develop a new empirical model of solar exergy that represents the local particular features, based solely on the clearness index k_t, since it is a parameter easily measured and allows taking into consideration the sky conditions.

2. Methodology

The exergy model of solar radiation was developed using the minute based data from a meteorological station located in Santiago, Chile. These data include measurements for the full year 2018, considering global horizontal radiation, horizontal diffuse radiation, direct normal radiation, wind velocity as well as ambient temperature. A filtering procedure was implemented, following the criteria proposed by Lemos et al (Lemos et al., 2017), aiming to eliminate any spurious data that could affect the subsequent analysis process. As Pons (2012) described in his work, the exergy of diffuse and direct solar radiation can be computed separately by dividing equation 3 into these two components:

$$b_{dr} = i_{dr} - T_0 j_{dr} \quad \text{(eq. 4)}$$
$$b_{df} = i_{df} - T_0 j_{df} \quad \text{(eq. 5)}$$

where b_{dr} is the direct exergy flux, i_{dr} the direct radiative flux and j_{dr} the direct entropy flux. Similarly, b_{df} is the diffuse exergy flux, i_{df} the diffuse radiative flux and j_{df} the diffuse entropy flux. The entropy flux is assumed as isotropic attenuation and uniform over the frequency spectrum. Then, the entropy flux is stated as,

$$j_{dr} = X_{dr}(\epsilon_{dr})\frac{4}{3}\frac{i_{dr}}{T_s} \quad \text{(eq. 6)}$$
$$j_{df} = X_{df}(\epsilon_{df})\frac{4}{3}\frac{i_{df}}{T_s} \quad \text{(eq. 7)}$$

where ϵ is the attenuation factor and $X_{dr}(\epsilon)$ is a function calculated numerically as,

$$X_{dr}(\epsilon_{dr}) = 0.973 - 0.275 \cdot \ln \epsilon + 0.0273\epsilon \quad \text{(eq. 8)}$$
$$X_{df}(\epsilon_{df}) = 0.9659 - 0.2776 \cdot \ln \epsilon \quad \text{(eq. 9)}$$
$$\epsilon_{dr} = \frac{\left(\frac{i_{dr}}{\omega_s \cos\theta}\right)}{\frac{\sigma T_s^4}{\pi}} \quad \text{(eq. 10)}$$
$$\epsilon_{df} = \frac{\left(\frac{i_{df}}{\pi}\right)}{\frac{\sigma T_s^4}{\pi}} \quad \text{(eq. 11)}$$

where ω_s is the incidence solid angle and is used as $6.79x10^{-5}(sr)$ and σ is the Stefan-Boltzmann constant. Finally, it is determined the exergy factor of global solar radiation ψ_{gl} by the sum of the factors of diffuse and direct solar radiation, as described by Neri et al. (Neri et al., 2017).

$$\psi_{gl} = \frac{b_{dr}+b_{df}}{i_{dr}+i_{df}} \quad \text{(eq. 12)}$$

From the regression analysis, it is explored the equation that can represent the exergy in terms of the clearness index k_t, which is determined using the meteorological data described above, and is easily computed for locations where accurate measurements are not available. Regarding the regression analysis, it is evaluated 13 different models such as: linear, quadratic, cubic, quartic, quintic, sextic, septic, logarithmic, exponential with one term (exponential 1), exponential with two terms (exponential 2), power with one term (power 1), power

with two terms (power 2), and inverse. Afterward, it is analyzed 10 different statistical error: Mean Bias Error (MBE), Mean Absolute Error (MAE), Root Mean Square Error (RMSE), Mean Percentage Error (MPE), Uncertainty at 95% (U_{95}), Relative Root Mean Square Error (RRMSE), t-statistics (t-stats), Maximum Absolute Relative Error (erMAX), Mean Absolute Relative Error (MARE) and Correlation Coefficient (R).

$$MBE = \frac{1}{n}\sum_{i=1}^{n}\left(\overline{H}_{i,e} - \overline{H}_{i,c}\right) \quad \text{(eq. 13)}$$

$$MAE = \frac{1}{n}\sum_{i=1}^{n}\left|\overline{H}_{i,e} - \overline{H}_{i,c}\right| \quad \text{(eq. 14)}$$

$$RMSE = \left[\frac{1}{n}\sum_{i=1}^{n}\left(\overline{H}_{i,e} - \overline{H}_{i,c}\right)^2\right]^{\frac{1}{2}} \quad \text{(eq. 15)}$$

$$MPE = \frac{1}{n}\sum_{i=1}^{n}\left(\frac{\overline{H}_{i,c} - \overline{H}_{i,e}}{\overline{H}_{i,c}}\right) \times 100 \quad \text{(eq. 16)}$$

$$U_{95} = 1.96(SD^2 + RMSE^2)^{\frac{1}{2}} \quad \text{(eq. 17)}$$

$$RRMSE = \frac{\sqrt{\frac{1}{n}\sum_{i=1}^{n}\left(\overline{H}_{i,c} - \overline{H}_{i,e}\right)^2}}{\sum_{i=1}^{n}\overline{H}_{i,c}} \quad \text{(eq. 18)}$$

$$t - stats = \left[\frac{(n-1)MBE^2}{RMSE^2 - MBE^2}\right]^{\frac{1}{2}} \quad \text{(eq. 19)}$$

$$erMAX = max\left(\left|\frac{\overline{H}_{i,c} - \overline{H}_{i,e}}{\overline{H}_{i,c}}\right|\right) \quad \text{(eq. 20)}$$

$$MARE = \frac{1}{n}\sum_{i=1}^{n}\left|\frac{\overline{H}_{i,e} - \overline{H}_{i,c}}{\overline{H}_{i,c}}\right| \quad \text{(eq. 21)}$$

$$R = \frac{\sum_{i=1}^{n}(\overline{H}_{i,e} - \overline{H}_{e,av})(\overline{H}_{i,c} - \overline{H}_{c,av})}{\sqrt{\sum_{i=1}^{n}\left(\overline{H}_{i,e} - \overline{H}_{e,av}\right)^2 \sum_{i=1}^{n}\left(\overline{H}_{i,c} - \overline{H}_{c,av}\right)^2}} \quad \text{(eq. 22)}$$

Considering that the statistical errors could differ in which model is the best to fit the data, it is used as an indicator that could discern using the 10 errors calculated. In this case it is used the indicator used by Jamil and Bellos (Jamil and Bellos, 2019). The Global Performance Indicator (GPI) described by Despotovic et al. (Despotovic et al., 2015) combines all the statistical errors into a single value, in which the greater the value is, the better the model performed in term of the behavior of the model into the data. First, it is normalized all the statistical errors on a scale of 0-1. Then, it is subtracted to the median of the respective scaled indicator. Afterward, the results are summed up after multiplying the valor with a weight factor indicate as follow,

$$GPI = \sum_{i=1}^{10}\alpha_j\left(\bar{y}_j - \bar{y}_{ij}\right) \quad \text{(eq. 23)}$$

$$\alpha_j = \begin{cases} -1, for\ correlation\ coefficient, R \\ +1, for\ all\ other\ statistical\ errors \end{cases} \quad \text{(eq. 24)}$$

where $\bar{y}_j$ is the median of the scaled values of the error j, $\bar{y}_{ij}$ is the scaled value of the statistical errors j for expression i.

2.1 Experimental verification

The expression found to be the best to fit the data is then validated by an experiment that consists of measuring different parameters in a photovoltaic panel, which allowed to determine the exergy factor of the solar radiation. The experimental set-up follows the criteria suggested by Akyuz et al. (Akyuz et al., 2012). The set-up considers a small photovoltaic panel of 10 (W) installed horizontally while is being measured different component described in Table 1. The instruments are connected to a datalogger CR300 from Campbell Scientific and the measurements are recorded minutely. The diagram with the variable evaluated is shown in Figure 1 and the experiment carried out to validate the expression can be seen in Figure 2.

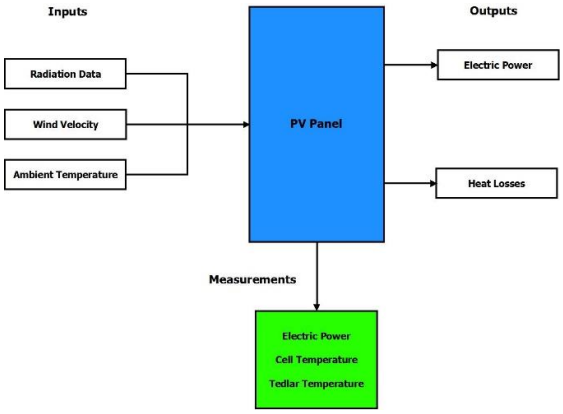

Fig. 1: Diagram with the inputs and outputs considered to develop the thermal and exergy model.

Fig. 2: Experimental setup evaluated.

Tab. 1: Measurement Variable in the photovoltaic panel

Measurement	Instrument	Unit
Wind velocity	Anemometer 03001 Young Wind Sentry Set, Campbell Scientific	m^2
Cell temperature	Thermocouple type k	K
Tedlar temperature	Thermocouple type k	K
Ambient temperature	CS-500, Campbell Scientifics	K
Solar radiation	Pyranometer CMP-22, Kipp&Zonen	W/m^2
Electric power	Microinverter M215, Enphase Energy	W

3. Results

The results of all the statistical errors for the different model evaluated are shown in Table 2. The lowest errors for every statistical value are colored in red and as can be seen in the table, every error offers a different view in which one is the best that suit the data used. The MBE has the lowest errors among the rest with values from 10^{-16} to 10^{-6}. The Linear, Quadratic, Cubic, fifth and sixth polynomials, Logarithmic, Exponential 2, Power 1 and Power 2 models do not show an acceptable fit, compared to the other models. The Fourth expression get the lowest MBE and t-stats with $-2.211 \cdot 10^{-16}$ and $2.493 \cdot 10^{-12}$. The seventh polynomial expression shows the best result for MAE, RMSE, MPE, RRMSE, erMAX and MARE. The Exponential expression with one term obtains a favorable result using the U_{95} and the Inverse expression develops the lowest errors using the R. With the different tendencies of the results, it is used the GPI to deliberate which one is the expression that best fit the data. In table 3 is observed the results for the GPI with the scaled values for every expression.

Furthermore, it a column with the result of the GPI and the ranking that every model obtains. As can be seen in table 3, the best model with the highest GPI is the seventh polynomial, with the following expression,

$$\psi_{go} = -58{,}4212 \cdot k_t^7 + 175{,}5171 \cdot k_t^6 - 194{,}7993 \cdot k_t^5 + 92{,}4632 \cdot k_t^4 - 13{,}1965 \cdot k_t^3 - 2{,}5353 \cdot k_t^2 + 1{,}0789 \cdot k_t + 0{,}6144 \quad \text{(eq. 25)}$$

To validate the representativity of this expression, it is used the experiment described in section 2. First, it is measured the variables written in Table 1 for a PV panel for four days of June in 2019 in Santiago de Chile. The measurements where complemented with a finite difference model implemented in Matlab, which allowed to compute the all the energy flows and the temperatures in all the layers of the PV system. The solver implemented in the model was the Crank Nicolson method, which is widely used to estimate the thermal behavior in one or two dimensions. For this case, considering the small size of the PV panel and its low electrical power, it is used the one-dimensional approach. To visualize the effectiveness of the model, it is represented a scatter plot that in figures 2, 3, and 4. The distribution of some points in Figure 4 behave as a vertical "line" is due to the resolution of the micro inverter M250 can only storage integer number. The normalized root mean squared error (NRMSE) for every scattering plot is calculated as,

$$NRMSE = \frac{1}{n}\left[\frac{1}{n}\sum_{i=1}^{n}\left(\bar{H}_{i,e} - \bar{H}_{i,c}\right)^2\right]^{\frac{1}{2}} \quad \text{(eq. 26)}$$

Tab. 2: Results of the different statistical errors for every model.

	MBE	MAE	RMSE	MPE	U95	RRMSE	t-stats	erMAX	MARE	R
Linear	-2.299E-15	2.776E-02	3.871E-02	-2.198E-01	1.008E-01	2.806E-07	2.349E-11	2.970E-01	3.280E-02	4.336E-01
Quadratic	1.485E-15	2.385E-02	3.598E-02	-1.866E-01	1.008E-01	2.608E-07	1.632E-11	2.914E-01	2.848E-02	5.108E-01
Cubic	-2.119E-15	2.302E-02	3.517E-02	-1.793E-01	1.008E-01	2.549E-07	2.383E-11	2.931E-01	2.732E-02	5.327E-01
Fourth	**-2.211E-16**	2.284E-02	3.507E-02	-1.783E-01	1.008E-01	2.542E-07	**2.493E-12**	2.913E-01	2.711E-02	5.351E-01
Fifth	-1.332E-14	2.284E-02	3.503E-02	-1.779E-01	1.008E-01	2.539E-07	1.504E-10	2.916E-01	2.710E-02	5.362E-01
Sixth	-6.863E-15	2.264E-02	3.493E-02	-1.768E-01	1.008E-01	2.532E-07	7.769E-11	2.899E-01	2.688E-02	5.389E-01
Seventh	2.062E-13	**2.259E-02**	**3.491E-02**	**-1.766E-01**	1.008E-01	**2.530E-07**	2.335E-09	**2.890E-01**	**2.682E-02**	5.394E-01
Logarithmic	3.657E-12	2.573E-02	3.773E-02	-2.059E-01	1.008E-01	2.734E-07	3.833E-08	4.436E-01	3.068E-02	4.621E-01
Exponential 1	1.678E-05	2.804E-02	3.908E-02	-2.285E-01	**1.003E-01**	2.833E-07	1.697E-01	2.966E-01	3.317E-02	4.227E-01
Exponential 2	-2.255E-06	2.325E-02	3.534E-02	-1.801E-01	1.009E-01	2.561E-07	2.523E-02	2.933E-01	2.765E-02	5.281E-01
Power 1	-4.664E-06	2.593E-02	3.750E-02	-2.027E-01	1.010E-01	2.718E-07	4.919E-02	3.218E-01	3.080E-02	4.685E-01
Power 2	-5.629E-15	2.604E-02	3.748E-02	-2.038E-01	1.008E-01	2.716E-07	5.940E-11	2.946E-01	3.088E-02	4.692E-01
Inverse	-5.419E-12	3.039E-02	4.584E-02	-3.079E-01	1.008E-01	3.322E-07	4.675E-08	1.478E+00	3.677E-02	**2.058E-01**

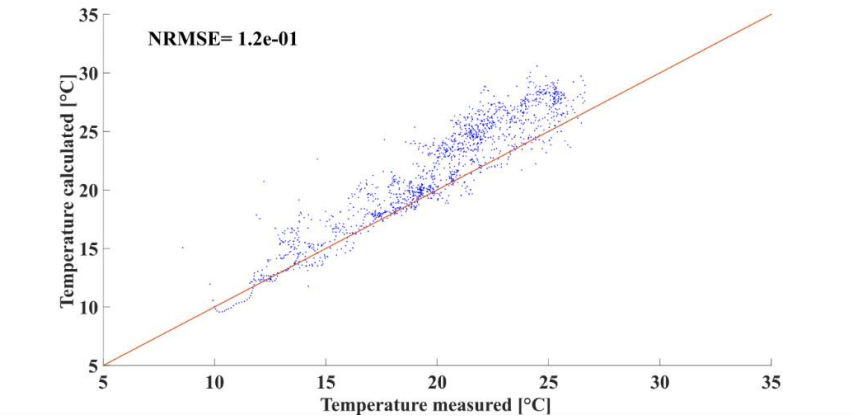

Fig. 3: Scatter plot of the temperature measured and calculated for the solar cell and their respective NRMSE.

Tab. 3: Scaled values of statistical errors and the rank of every expression.

	MBE	MAE	RMSE	MPE	U95	RRMSE	t-stats	erMAX	MARE	R	GPI	Rank
Linear	2.175E-01	6.627E-01	3.480E-01	6.709E-01	7.831E-01	3.480E-01	1.237E-10	6.765E-03	6.006E-01	6.827E-01	-1.417E+00	11
Quadratic	2.175E-01	1.614E-01	9.781E-02	9.238E-01	7.831E-01	9.781E-02	8.144E-11	2.075E-03	1.664E-01	9.141E-01	1.601E-03	7
Cubic	2.175E-01	5.478E-02	2.337E-02	9.796E-01	7.831E-01	2.337E-02	1.257E-10	3.465E-03	4.989E-02	9.797E-01	3.820E-01	5
Fourth	2.175E-01	3.096E-02	1.485E-02	9.869E-01	7.831E-01	1.485E-02	0	1.974E-03	2.939E-02	9.871E-01	4.449E-01	4
Fifth	2.175E-01	3.189E-02	1.128E-02	9.903E-01	7.831E-01	1.128E-02	8.711E-10	2.201E-03	2.820E-02	9.902E-01	4.519E-01	3
Sixth	2.175E-01	5.322E-03	1.886E-03	9.983E-01	7.831E-01	1.886E-03	4.430E-10	7.427E-04	5.801E-03	9.984E-01	5.212E-01	2
Seventh	2.175E-01	0	0	1	7.831E-01	0	1.374E-08	0	0	1	5.368E-01	**1**
Logarithmic	2.175E-01	4.020E-01	2.578E-01	7.768E-01	7.831E-01	2.578E-01	2.258E-07	1.301E-01	3.882E-01	7.681E-01	-9.077E-01	9
Exponential 1	1	6.990E-01	3.819E-01	6.047E-01	0	3.819E-01	1	6.373E-03	6.378E-01	6.501E-01	-2.524E+00	12
Exponential 2	1.124E-01	8.389E-02	3.910E-02	9.736E-01	8.880E-01	3.910E-02	1.486E-01	3.666E-03	8.292E-02	9.660E-01	1.321E-01	6
Power 1	0	4.273E-01	2.370E-01	8.015E-01	1	2.370E-01	2.898E-01	2.758E-02	3.997E-01	7.875E-01	-1.095E+00	10
Power 2	2.175E-01	4.414E-01	2.347E-01	7.929E-01	7.831E-01	2.347E-01	3.353E-10	4.733E-03	4.080E-01	7.896E-01	-7.901E-01	8
Inverse	2.175E-01	1	1	0	7.830E-01	1	2.754E-07	1	1	0	-4.463E+00	13

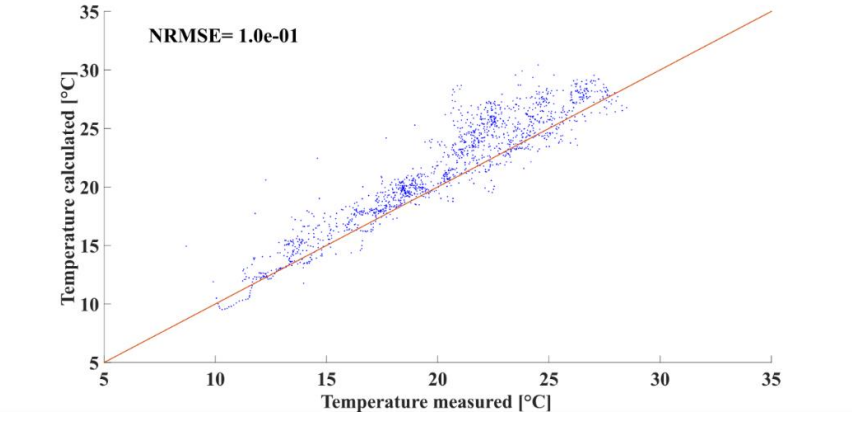

Fig. 4: Scatter plot of the temperature measured and calculated for the tedlar and their respective NRMSE.

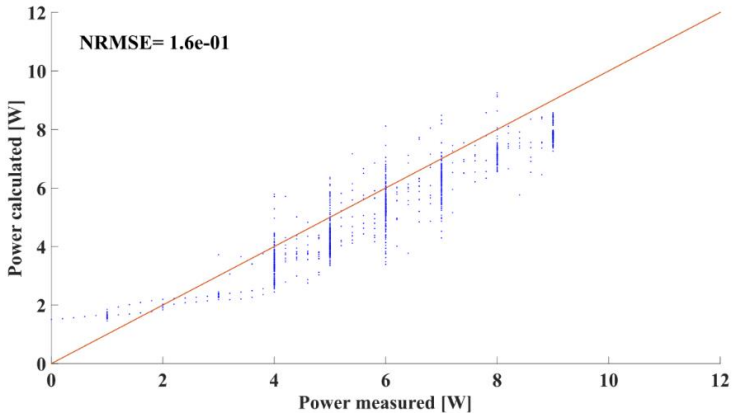

Fig. 5: Scatter plot of the power measured and calculated for the PV panel and their respective NRMSE.

Figure 2 and 3 show that the estimated values of the temperature for the solar cell and Tedlar, respectively, which effectively correlates the measured data. The NRMSE for both the solar cell and Tedlar is 0.12 and 0.10 respectively, which means that the estimated values fit the measured data. As observed in Figure 4, the power measured and the power calculated have a NRMSE of 0.16, which is explained by the limited resolution on the microinverter, as previously mentioned. Both figures of temperatures show that the calculated values are higher the measured data, and the electrical power of the PV panel behave as the opposite, where the measured data obtained highest values than the power calculated from the thermal model. Now, it is used the data calculated to obtain the exergy of the system, which is calculated as follow,

$$\sum \dot{Ex}_{in} = \sum \dot{Ex}_{out} \quad \text{(eq. 27)}$$

where,

$$Ex_{in} = Ex_{rad} \quad \text{(eq. 28)}$$

$$Ex_{out} = Ex_{elec} + Ex_{th} + Ex_{dest} \quad \text{(eq. 29)}$$

where the input exergy is considered as the exergy of the radiation Ex_{rad} and the output exergy is the electrical and thermal exergy. All the irreversibilities in the system are considered exergy destruction Ex_{dest} and cannot be measured. The electrical and thermal exergy is expressed as follows,

$$Ex_{elec} = V_m I_m \quad \text{(eq. 30)}$$

$$Ex_{th} = \left(1 - \frac{T_0}{T_{cell}}\right)\dot{Q} \quad \text{(eq. 31)}$$

where the heat flow $\dot{Q}$ is computed from the thermal analysis above. Rearranging the term of equation 28 and 29 in 27, it is obtained,

$$Ex_{rad} = Ex_{elec} + Ex_{th} + Ex_{dest} \quad \text{(eq. 32)}$$

and finally, dividing this equation with Ex_{rad}, it is obtained the exergy factor of the system ψ_{sys},

$$\psi_{sys} = \frac{Ex_{elec}+Ex_{th}}{Ex_{rad}} \quad \text{(eq. 33)}$$

$$\psi_{sys} = \frac{V_m I_m + \left(1-\frac{T_0}{T_{cell}}\right)\dot{Q}}{Ex_{rad}} \quad \text{(eq. 34)}$$

The destruction exergy Ex_{dest} was omitted in our analysis. To compare the model proposed in equation 25 with the one obtained in the literature, the radiation exergy Ex_{rad} will be used as described from the classic approach by Petela's model (Petela, 1964) and Zamfirescu & Dincer's model (Zamfirescu and Dincer, 2009), equation 1 and 2 respectively. The result for a sample day of June in 2019 can be seen in figure 5, 6 and 7.

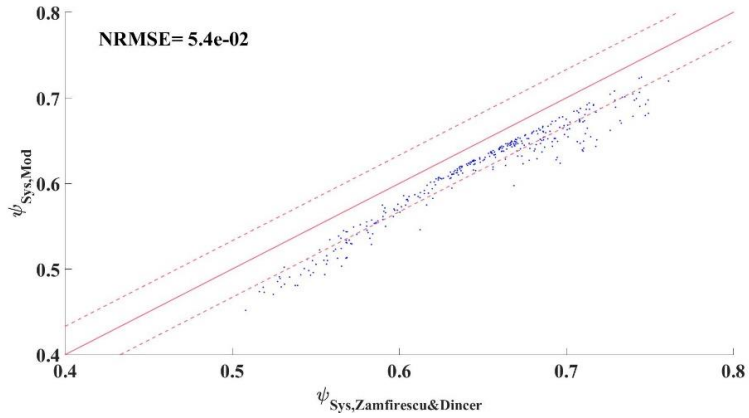

Fig. 6: Comparison between the model proposed and Zamfirescu & Dincer's model with their respective NRMSE.

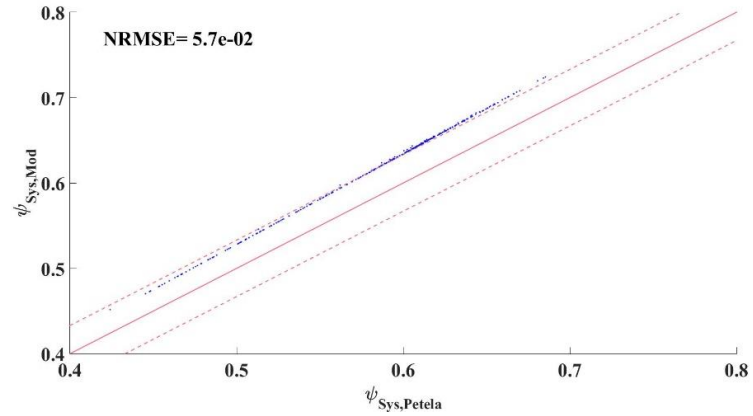

Fig. 7: Comparison between the model proposed and Petela's model with their respective NRMSE.

In figures 5, 6 and 7 it is observed that the exergy factor obtained by using equation 34 for the different models. First, the exergy factor calculated using Zamfirescu & Dincer's Model shows values above the model proposed. Also, most of the points are in the region delimited as the standard deviation limits for all the figures. For the day evaluated, the exergy factors are in the range approximately 0.45 to 0.75 in a day of Winter, with the highest concentration of points between 0.6 to 0.7 and the NRMSE was 0.054. in figure 6 it obtained the opposite tendencies of figure 5. Here, the model proposed obtained highest values than the Petela's model. Also, above $\psi_{Sys,Petela} = 0.6$ the data exceed the superior limit, which means that with highest solar radiation the difference between the model proposed and Petela´s model increased. The NRMSE was 0.057, higher than the one obtained from Figure 5. Figure 7 shows the model proposed compared to Pons's model which was the model used as base to obtain the model proposed. It can be expected that the difference between both models would be small and this is clearly represented with an NRMSE of 0.0015. To sum up, the model proposed is located between Petela's and Zamfirescu & Dincer's models, with a tendency to be closer to Zamfirescu & Dincer's model for the sample day.

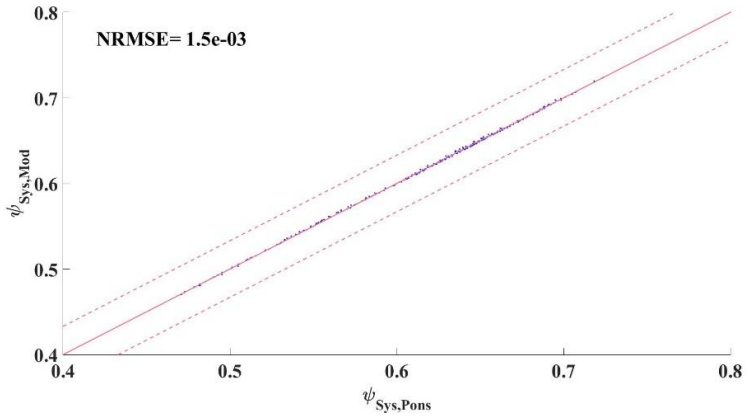

Fig. 8: Comparison between the model proposed and Pons's model with their respective NRMSE.

4. Conclusions

The exergy of solar radiation is one of the most important topics to solve in every solar plant because it can estimate the real work obtainable from the solar resource. Therefore, an expression that obtain the solar radiation exergy that could be reliable and be validated with real data is important for every exergy balance in a solar plant. In this work, the main purposed was to obtain an expression of the solar radiation exergy created with the particular meteorological condition in Santiago de Chile. This expression was obtained from a meteorological station of the complete year 2018. The seventh expression obtained the best result among the thirteen different expressions proposed thanks to an evaluation with ten kinds of statistical errors. Then, it is used an indicator to deliver the best model with the use of the GPI. Moreover, the seventh expression was the one who obtained the highest GPI. Afterward, it is compared the model proposed with the one widely used in the literature: Petela's model and the new approach proposed by Zamfirescu & Dincer.

An experiment is evaluated with the condition suggested by Akyuz et al. (Akyuz et al., 2012). It is used as a PV panel, where every variable is measured on a minute basis, which was combined to the implementation of a thermal model. The thermal model presents low NRMSE for every variable. The data obtained from thermal model was used as input for the comparison of the proposed exergy model, and the other solar radiation exergy models described above. The model proposed obtained closer results to Zamfirescu & Dincer rather than Petela´s model. The radiation exergy Ex_{rad} was overestimated in the Petela's model, and Zamfirescu & Dincer obtained lowest result in comparison with the model proposed. The NRMSE obtained for the comparison was representative of these differences stated above. Finally, the model proposed it could be used with data of different sites of the country and evaluate the radiation exergy especially in the north of Chile, where this expression could be used as an input for an exergy balance in different kind of solar applications.

5. Acknowledgments

The authors would like to thank the support of the Solar Energy Research Center (SERC Chile) for the financial support for this work.

6. References

Akyuz, E., Coskun, C., Oktay, Z., Dincer, I., 2012. A novel approach for estimation of photovoltaic exergy efficiency. Energy 44, 1059–1066. https://doi.org/10.1016/j.energy.2012.04.036

Despotovic, M., Nedic, V., Despotovic, D., Cvetanovic, S., 2015. Review and statistical analysis of different global solar radiation sunshine models. Renew. Sustain. Energy Rev. 52, 1869–1880. https://doi.org/10.1016/j.rser.2015.08.035

Escobar, R.A., Cortés, C., Pino, A., Salgado, M., Pereira, E.B., Martins, F.R., Boland, J., Cardemil, J.M., 2015. Estimating the potential for solar energy utilization in Chile by satellite-derived data and ground station measurements. Sol. Energy 121, 139–151. https://doi.org/10.1016/j.solener.2015.08.034

Gribik, J.A., Osterle, J.F., 1984. The second law efficiency of solar energy conversion. Sol. Energy 106, 553. https://doi.org/10.1016/0038-092X(81)90168-7

Jamil, B., Bellos, E., 2019. Development of empirical models for estimation of global solar radiation exergy in India. J. Clean. Prod. 207, 1–16. https://doi.org/10.1016/j.jclepro.2018.09.246

Jeter, S.M., 1981. Maximum conversion efficiency for the utilization of direct solar radiation. Sol. Energy 26, 231–236. https://doi.org/10.1016/0038-092X(81)90207-3

Lemos, L.F.L., Starke, A.R., Boland, J., Cardemil, J.M., Machado, R.D., Colle, S., 2017. Assessment of solar radiation components in Brazil using the BRL model. Renew. Energy 108, 569–580. https://doi.org/10.1016/j.renene.2017.02.077

Neri, M., Luscietti, D., Pilotelli, M., 2017. Computing the Exergy of Solar Radiation From Real Radiation Data. J. Energy Resour. Technol. 139, 061201. https://doi.org/10.1115/1.4036772

Petela, R., 1964. Exergy of Heat Radiation. J. Heat Transfer 86, 187. https://doi.org/10.1115/1.3687092

Pons, M., 2012. Exergy analysis of solar collectors, from incident radiation to dissipation. Renew. Energy 47, 194–202. https://doi.org/10.1016/j.renene.2012.03.040

Raugei, M., Leccisi, E., Fthenakis, V., Escobar Moragas, R., Simsek, Y., 2018. Net energy analysis and life cycle energy assessment of electricity supply in Chile: Present status and future scenarios. Energy 162, 659–668. https://doi.org/10.1016/j.energy.2018.08.051

Zamfirescu, C., Dincer, I., 2009. How much exergy one can obtain from incident solar radiation? J. Appl. Phys. 105. https://doi.org/10.1063/1.3081637